Journal of Chromatography A, 1228 (2012) 221–231

Contents lists available at SciVerse ScienceDirect

Journal of Chromatography A

journal homepage: www.elsevier.com/locate/chroma

Evaluation of columns packed with shell particles with compounds of pharmaceutical interest

Joséphine Ruta[1], Daria Zurlino[1], Candice Grivel[2], Sabine Heinisch[2], Jean-Luc Veuthey[1], Davy Guillarme[1,*]

[1] School of Pharmaceutical Sciences, University of Geneva, University of Lausanne, Bd d'Yvoy 20, 1211 Geneva 4, Switzerland
[2] Laboratoire des Sciences Analytiques, UMR CNRS 5180, Université de Lyon, 43 Boulevard du 11 Novembre 1918, 69622 Villeurbanne Cedex, France

ARTICLE INFO

Article history:
Available online 12 September 2011

Keywords:
Fused-core
Core–shell
Shell
Superficially porous particles
Pharmaceutical
UHPLC
UPLC

ABSTRACT

The commercial C18 columns packed with sub-3 μm shell particles were tested and compared to a reference UHPLC column, in terms of kinetic performance as well as selectivity, retention capability, peak shape and loading capacity. For this purpose, a set of pharmaceutically relevant molecules was selected, including acidic, neutral and basic drugs. Regarding kinetic performance, h_{opt} values for the shell particles were found between 1.7 and 2, while the UHPLC column provided a value of approximately 2.5. However, this impressive performance should be considered with caution, particularly for the construction of kinetic plots since h_{opt} values were sometimes related to the column dimensions, depending on the provider (h_{opt} comprised between 1.8 and 2.6 for longer columns of 150 mm packed with shell particles). Despite the non-porous inner core of the shell particles representing between 25 and 36% of the particle, we demonstrated that the decrease in retention was on the maximum equal to 15% for Ascentis column while Acquity and Poroshell were strictly equivalent in terms of retention. Concerning loading capacity, it remains comparable to that of fully porous sub-2 μm particles and always more pronounced with 0.1% formic acid *vs.* phosphate buffer. The loading capacity of the different columns was found to be better correlated to the pore volume or surface coverage than the shell thickness. Experimentally, the most pronounced overloading was observed with the Poroshell. Finally, the selectivity and peak shape were evaluated using a mixture of basic and acidic drugs. It appears that results were very similar between sub-3 μm shell particles and fully porous sub-2-μm particles for our mixture of compounds, showing the ability to transfer existing methods to shell particles, with only limited adjustments. This study confirms the potential of columns packed with shell particles and demonstrates the interest of such column technology with pharmaceutical compounds.

1. Introduction

In modern LC, columns packed with shell particles can be of interest to meet requirements in terms of throughput and elevated resolution [1,2]. During the 1960s, Horvath et al. pioneered work on pellicular particles, but there was not a strong interest from the chromatographic community because it was exclusively ion-exchange material. In the 1980s, Unger et al. prepared pellicular particles made of C18 material, but the loading capacity was too limited [3]. In 1992, Kirkland [4] reported the successful synthesis of core–shell particles with a larger shell thickness (i.e., the particles on average measured 7 μm, with a 1 μm shell thickness), allowing sufficient retention and loading capacity. Later, these columns were commercialized by Agilent with 5 μm particles under the name Poroshell 300 Å. However, their success was limited because these columns were mostly dedicated to the analysis of peptides and proteins, but other techniques were generally employed for the analysis of biomolecules at the end of the 1990s [5].

Finally, the most recent development of shell particles was introduced in 2007 by a company founded by J.J. Kirkland, Advanced Material Technologies (Wilmington, DE, USA), under the trademark Halo [6]. This new version of shell particles was markedly improved in terms of its chromatographic performance. In addition, the particle size was drastically reduced to 2.7 μm to meet the requirement for high throughput and high-resolution separations, while the porous shell thickness should remain suitable (0.5 μm) for retention and loading capacity [7]. In terms of marketing, this new packing material was primarily dedicated to the analysis of small molecular weight compounds but could also be employed for peptides and proteins, which is currently a field of interest for RPLC. Today,

* Corresponding author at: School of Pharmaceutical Sciences, University of Geneva, Bd d'Yvoy 20, 1211 Geneva 4, Switzerland. Tel.: +41 22 379 34 63; fax: +41 22 379 68 08.
E-mail address: davy.guillarme@unige.ch (D. Guillarme).

0021-9673/$ – see front matter © 2011 Elsevier B.V. All rights reserved.
doi:10.1016/j.chroma.2011.09.013

various columns packed with sub-3-μm shell particles are commercialized, including Ascentis from Supelco (Bellefonte, PA, USA), Kinetex from Phenomenex (Torrance, CA, USA) and more recently Poroshell from Agilent (Waldbronn, Germany). Currently, columns are available with particle sizes of 1.7, 2.6 or 2.7 μm and porous shell thickness equal to 0.23, 0.35 and 0.5 μm, respectively [8].

A survey on recent literature related to shell particle technology has demonstrated that most of the works deal with the kinetic performance evaluation of such columns using model compounds and analytical conditions far from those commonly employed in application laboratories [9,10]. In addition, there is only one paper published in the meantime of this study [11] that refers to the overloading behavior of sub-3-μm shell particles. The goal of the present study, was to evaluate the columns packed with sub-3-μm shell particles commercially available in terms of their kinetic performance, retention capability, loading capacity, selectivity and peak shape. Thus, to assess the potential of these columns, compounds of pharmaceutical interest were examined using the gradient mode and pH conditions close to procedures commonly employed by the pharmaceutical industry.

2. Experimental

2.1. Chemical and reagents

Water was obtained from a Milli-Q Water Purification System from Millipore (Bedford, MA, USA). Acetonitrile and methanol were of HPLC gradient grade from Panreac Quimica (Barcelona, Spain). Ammonium hydroxide and potassium dihydrogen phosphate (KH_2PO_4) were from Sigma-Fluka (Buchs, Switzerland). Formic acid was of ULC–MS grade and purchased from Biosolve (Valkenswaald, Netherlands). Dipotassium hydrogen phosphate (K_2HPO_4) was from Riedel-de-Haën (Seelze, Germany).

Methylparaben, ethylparaben, propylparaben, butylparaben, uracil, morphine, atenolol, codeine, lidocaine, prilocaine, acebutolol, bupropion, bupivacaine, propranolol, trimipramine, ketoprofen, flurbiprofen, ibuprofen, sulfaguanidine, and sulfadiazine were supplied by Sigma-Fluka and sulfanilamide was purchased from Merck (Darmstadt, Germany).

A stock solution of uracil, methylparaben, ethylparaben, propylparaben and butylparaben at 25 mg/mL in methanol was prepared and diluted in water to obtain a final solution at 50 μg/mL. For the analysis of the 13 test compounds, all samples were prepared by an appropriate dilution of a 1 mg/mL stock solution of each compound in MeOH to obtain the desired concentration in water:methanol (80:20, v/v). Aqueous sulfonamides mixture at 50 μg/mL in water was prepared from a stock solution at 300 μg/mL.

For the analysis performed at pH 2.7, 0.1% formic acid was added to both water and ACN. Concerning the study at pH 6.85, a phosphate buffer at 20 mM was prepared using an adequate quantity of K_2HPO_4 and KH_2PO_4 solutions at 20 mM to reach the desired pH.

2.2. Instrumentation

Chromatographic experiments were performed using a Waters Acquity ultra performance liquid chromatography (UPLC) system (Waters, Milford, MA, USA) that can deliver mobile phases at pressures up to 1000 bar. This instrument was equipped with a binary solvent manager with a maximum delivery flow rate of 2 mL/min, a sample manager with a 2, 5 and 10 μL loop for the analysis performed on 50, 100 and 150 mm columns length, respectively (injections performed in full-loop conditions), a UV–vis programmable detector with a 500 nL flow cell, and a column manager composed of a column oven and a pre-column heater. Data acquisition, data handling, and instrument control were performed by Empower Software v2.0. The UV wavelength was set at 240 nm for parabens analysis and 230 nm for the other mixtures. The acquisition rate and time constant were systematically fixed at 20 Hz and 50 ms for all compounds. The extra column volume, (V_{ext}), and the dwell volume (V_d), were experimentally measured at 13 and 100 μL, respectively with the 2 μl injection loop.

Table 1 summarized the properties of columns tested during this study. It is important to mention here that the Ascentis Express C18 and Halo C18 columns should theoretically be the same. Indeed this stationary phase is produced by Advanced Materials Technology who sells this column under the name of Halo, while Supelco is a vendor of this phase with another name, Ascentis Express. However, as exposed in this study, some significant differences can be observed between these two materials and we can express some doubts about their equivalency.

2.3. Kinetic plot

To evaluate the kinetic performance of different columns, a kinetic plot methodology was applied to simultaneously account for the mobile phase flow rate, chromatographic efficiency, generated backpressure and column geometry. This methodology was based on the work of Desmet et al. [12] according to Eqs. (1) and (2):

$$N = \frac{\Delta P_{max}}{\eta}\left(\frac{K_{v0}}{u \cdot H}\right)_{experimental} \quad (1)$$

$$t_0 = \frac{\Delta P_{max}}{\eta}\left(\frac{K_{v0}}{u^2}\right)_{experimental} \quad (2)$$

The above equations include experimental Van Deemter data (u, H), permeability values (K_{v0}), a scaling value for the pressure drop (ΔP), which was fixed at 600 bar for shell particles and 1000 bar for fully porous sub-2-μm particles, and the mobile phase viscosity (η), which was equal to 0.76 cP for a mobile phase containing 35:65 ACN:H_2O at 40 °C [13]. Thus, both equations were employed to transform experimental data into extrapolated plots of analysis time *vs.* efficiency. This can be done automatically using an excel tool developed by Desmet group (kinetic plot analyzer), available on the web [14]. For more information on kinetic plot construction, readers can refer to [15].

3. Results and discussion

3.1. Kinetic performance of shell particles

To evaluate the kinetic performance of a chromatographic system, experimental values of efficiencies at various mobile phase linear velocities should be fitted with the well-known Van Deemter equation:

$$H = A + \frac{B}{u} + Cu \quad (3)$$

where H is the height equivalent to a theoretical plate, u is the mobile phase linear velocity and A, B and C terms are constant, accounting for band broadening. The A coefficient represents the eddy dispersion, the B term is the longitudinal diffusion and the C parameter is related to mass transfer resistances.

The kinetic performance of columns packed with shell particles has been extensively investigated by Gritti and Guiochon [16–18]. Most of their studies were dedicated to the evaluation of Kinetex material using model compounds. In another study, Desmet et al. [19] made a comparison of separation efficiencies that can be attained with various commercial columns packed with shell particles, including Kinetex, Halo and Poroshell materials. Finally, Fekete et al. also made important contribution to the kinetic evaluation of this new technology [20,21]. These authors reported very

Table 1
Column properties.

Column name	Suppliers	Particle diameter (μm)	Porous diameter (μm)	Non-porous diameter (μm)	Pore size (Å)	pH range	Endcapping?	ΔP_{max} (bar)	T_{max} (°C)
Acquity UPLC BEH C18	Waters	1.7	1.7	–	130	1–12	Yes	1000	90
Poroshell 120 EC-C18	Agilent	2.7	0.5	1.7	120	2–9	Yes	600	60
Ascentis Express C18	Supelco	2.7	0.5	1.7	90	2–9	Yes	600	60
Kinetex C18	Phenomenex	2.6	0.35	1.9	100	1.5–10	Yes	600	60
Halo C18	AMT	2.7	0.5	1.7	90	2–9	Yes	600	60

small *h* values (reduced height equivalent to a theoretical plate) for small, uncharged compounds to 1.5 [7] and below (1 [9]) for such columns, in contrast to values of 2–3 for columns packed with porous particles. The main conclusions on the van Deemter terms to explain this behavior was the following: (i) the diffusion path is shorter compared to totally porous particles because the inner core is solid, and thus, impenetrable by analytes. The C-term is then reduced but not dramatically, and therefore, it cannot explain the outstanding kinetic performance of shell particles. (ii) Because it is possible to precisely control the shell thickness of this material, these columns present an exceptionally narrow particle size distribution in addition to an enhanced roughness of their surface compared to porous particles, leading to a smaller A-coefficient by about 40%. (iii) The presence of the solid core also has a direct consequence on the *B*-value because analytes cannot axially diffuse in the solid inner core. As reported by Guiochon and Gritti, the *B*-term decreases by approximately 20% between a fully porous and a shell particle [3]. Finally, for small neutral molecules, the semi-porous particles maintain approximately 80% efficiency of sub-2-μm particles but with a 2-fold lower backpressure for an identical column length [1].

3.2. Van Deemter curves and pressure plots

Van Deemter curves were plotted in Fig. 1A for the four different columns packed with shell particles and for UHPLC columns with the same length (50 mm). The u_{opt} values were comprised between 3 and 4 mm/s for butylparaben ($k \approx 8$), while optimal plate heights ranged between 4 and 6 μm. The Acquity column was the most efficient, with a H_{opt} value 10% better than the best shell particles column, i.e., the Poroshell. The differences between Poroshell, Ascentis and Kinetex were negligible, with H_{opt} values ranging between 4.64 and 4.79 μm (see Table 2). Finally, the Halo column produced a significantly lower kinetic performance (H_{opt} value of 5.39 μm). Despite the lower performance of the Halo column, when taking into account the particle size of the supports, h_{opt} values were always below 2 for columns packed with shell particles, while the Acquity produced an acceptable but significantly higher h_{opt} value (h_{opt} = 2.52) confirming recently published data [20].

HPLC columns are generally divided into "batches" of stationary phases and "lots" of columns. Thus, two types of problem can be encountered with this quite new technology and have not yet been discussed in the literature: (i) the packing material is not consistent between columns/batches: problem of batch-to-batch reproducibility and (ii) the different column geometries/lots are not well packed. In other words, the packing quality could vary with the column geometry, and thus, it could be beneficial to also evaluate various column lengths. Because of the substantial price of these columns, it was difficult to have three columns from different batches at our disposal, with three different lengths and from five different providers. Thus, this study was limited to a reasonable number of columns, including Poroshell and Kinetex columns with variable lengths (50, 100 and 150 mm) and only to the evaluation of the packing quality. Because the number of column of each dimension was very limited (n = 1), the preliminary data presented here should be considered with caution. The corresponding results are reported in Fig. 2A and 2B, respectively. As expected, the inter-column variability for different columns lengths from the same chemistry was quite high, i.e., H_{opt} varied between 4.6 and 5.5 μm for the Poroshell column, and between 4.8 and 6.9 μm for the Kinetex column. In this context, results reported in Figs. 1 and 2 should be interpreted with caution because a strong variation of efficiency between columns of different lengths was observed. Based on these experiments, it was

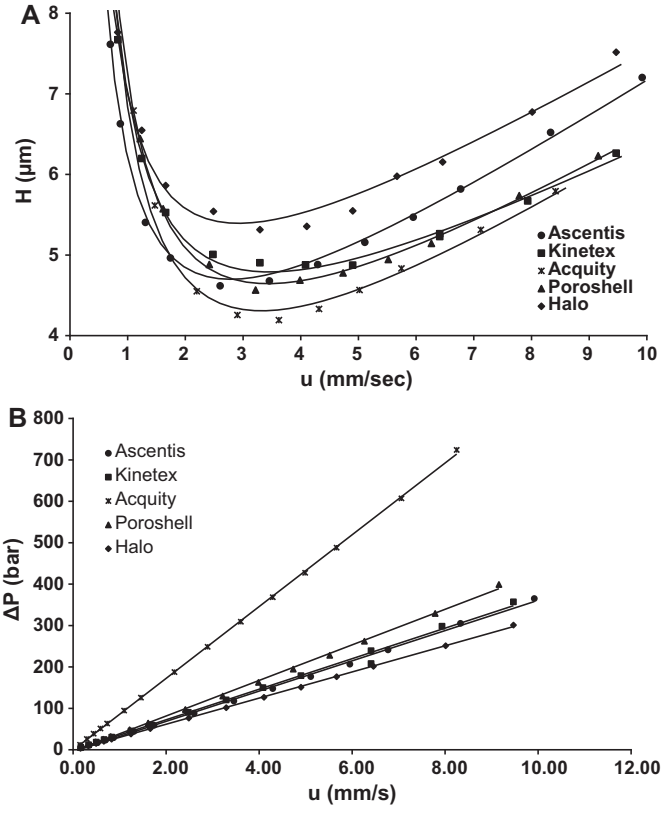

Fig. 1. (A) Dependencies of theoretical plate height (*H*) on linear velocity (*u*) obtained for butylparaben (50 μg/mL) with different stationary phases. Columns: Ascentis Express C18, 50 × 2.1 mm, 2.7 μm; Kinetex C18, 50 × 2.1 mm, 2.6 μm; Acquity BEH C18, 50 × 2.1 mm, 1.7 μm; Poroshell 120 EC-C18, 50 × 2.1 mm, 2.7 μm and Halo C18, 50 × 2.1 mm, 2.7 μm. *Conditions*: isocratic conditions of acetonitrile: water (35:65, v/v) were used for all columns excepted for Kinetex and Poroshell columns where acetonitrile:water (34:66, v/v) and acetonitrile:water (36:64, v/v) were used respectively, injected volume = 2 μL, λ = 240 nm, T = 40 °C and different flow rates from 20 to 1200 μL/min were tested to construct Van Deemter curves. To improve readability, the *Y*-axis was cut at H = 8 μm and thus, the H values observed at lowest mobile phase flow rates were not always reported. (B) Evolution of pressure in function of the mobile phase flow rate for all columns.

Table 2
chromatographic parameters of the columns.

Column name	Particles diameter (μm)	50 mm column length					150 mm column length			
		u_{opt} (mm/s)	H_{opt} (μm)	h_{opt}	K_{t0} (m^2)	E	H_{opt} (μm)	h_{opt}	K_{t0} (m^2)	E
Acquity	1.7	3.40	4.30	2.52	4.39 E^{-15}	4250	4.61	2.71	5.28 E^{-15}	4020
Poroshell 120 EC	2.7	3.50	4.64	1.71	8.85 E^{-15}	2430	5.50	2.04	1.11 E^{-14}	2720
Ascentis Express	2.7	2.97	4.70	1.74	1.04 E^{-14}	2120	–	–	–	–
Kinetex	2.6	3.57	4.79	1.84	1.03 E^{-14}	2220	6.91	2.66	1.20 E^{-14}	3980
Halo	2.7	2.96	5.39	1.99	1.20 E^{-14}	2420	4.93	1.83	1.49 E^{-14}	1630

$\left(h_{opt} = \frac{H_{opt}}{d_p} \text{ and } E = \frac{H^2_{opt}}{K_{t0}}\right)$.

impossible to conclude whether the efficiency loss was attributed to batch-to-batch variability or to a packing problem with longer columns. However, these preliminary results highlight the need to duplicate experiments with various columns packed with shell particles from the same provider before drawing conclusions. Furthermore, providers still need to improve the packing procedure for all geometries.

Finally, 50 mm columns packed with shell particles provided a reduction of efficiency by only 7–20% compared to the reference UHPLC 50-mm column packed with sub-2 μm particles. For the 150 mm column length, the reduction of efficiency was between 6 and 33% compared to the Acquity column. However, a simultaneous significant reduction of backpressure was also observed, as shown in Fig. 1B. The pressure drop was reduced by 1.8- to 2.4-fold, highlighting the benefits of 2.6 or 2.7 μm shell particles. For example, the pressure drop for a mobile phase flow rate of 1 mL/min was equal to 607, 329, 305, 298 and only 251 bar on Acquity, Poroshell, Ascentis, Kinetex and Halo columns, respectively. Finally, because of the reasonable generated backpressure, columns packed with shell particles could theoretically be compatible with a conventional HPLC system, provided that (i) the extra-column contributions and system dwell volume were minimized, (ii) methanol–water mixtures were not employed because viscosity is approximately 2-fold higher than acetonitrile–water mixtures, (iii) long columns providing high resolution are not required.

Another figure of merit widely employed for column comparison is the separation impedance, E which describes the tradeoff between speed, efficiency and pressure. The latter was calculated and reported in Table 2. As expected, the impedance of 50 mm column packed with sub-2 μm particles was equal to 4250 while all the 50 mm length columns packed with shell particles possess E values between 2100 and 2400, because of the very impressive h values.

3.3. Kinetic plots

Another way to illustrate the data reported in Figs. 1 and 2 is the kinetic plots representation. As described in the experimental

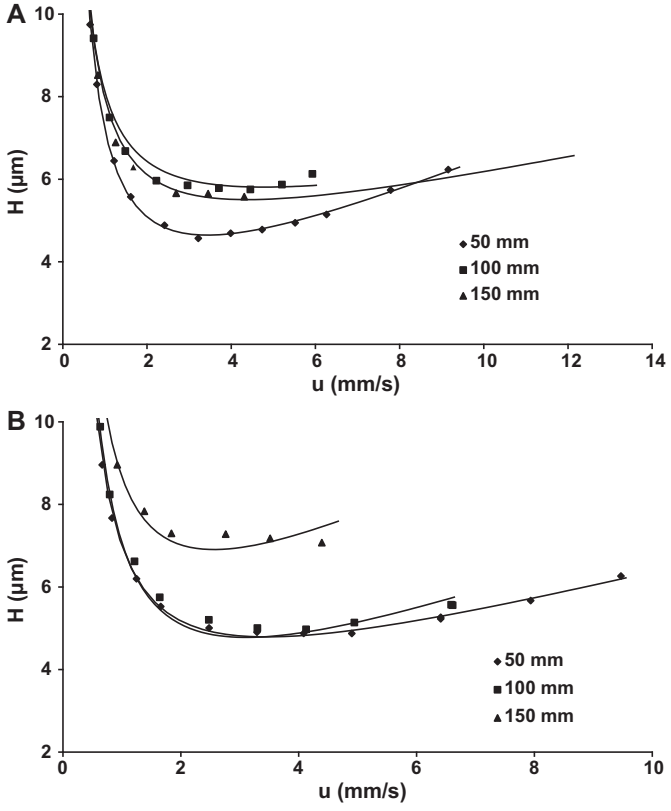

Fig. 2. Van Deemter curves for Poroshell (A) and Kinetex (B) columns of different length (50, 100, and 150 mm) obtained in the same conditions of Fig. 1.

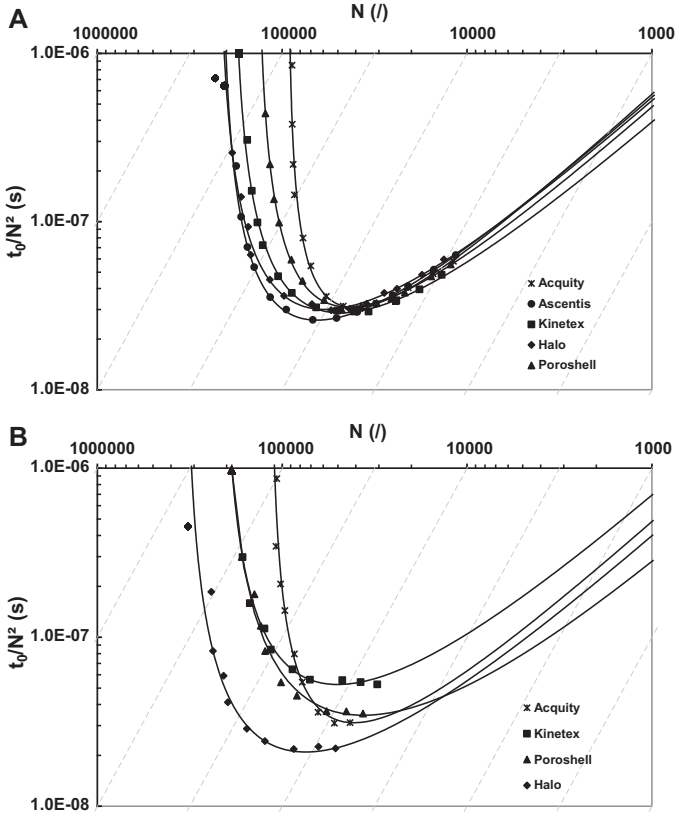

Fig. 3. Performance comparison of various stationary phases using kinetic plots representation: $t_0/N^2 = f(N)$ for butylparaben with the 50 mm length (A) and the 150 mm length (B) columns in the same conditions as in Fig. 1.

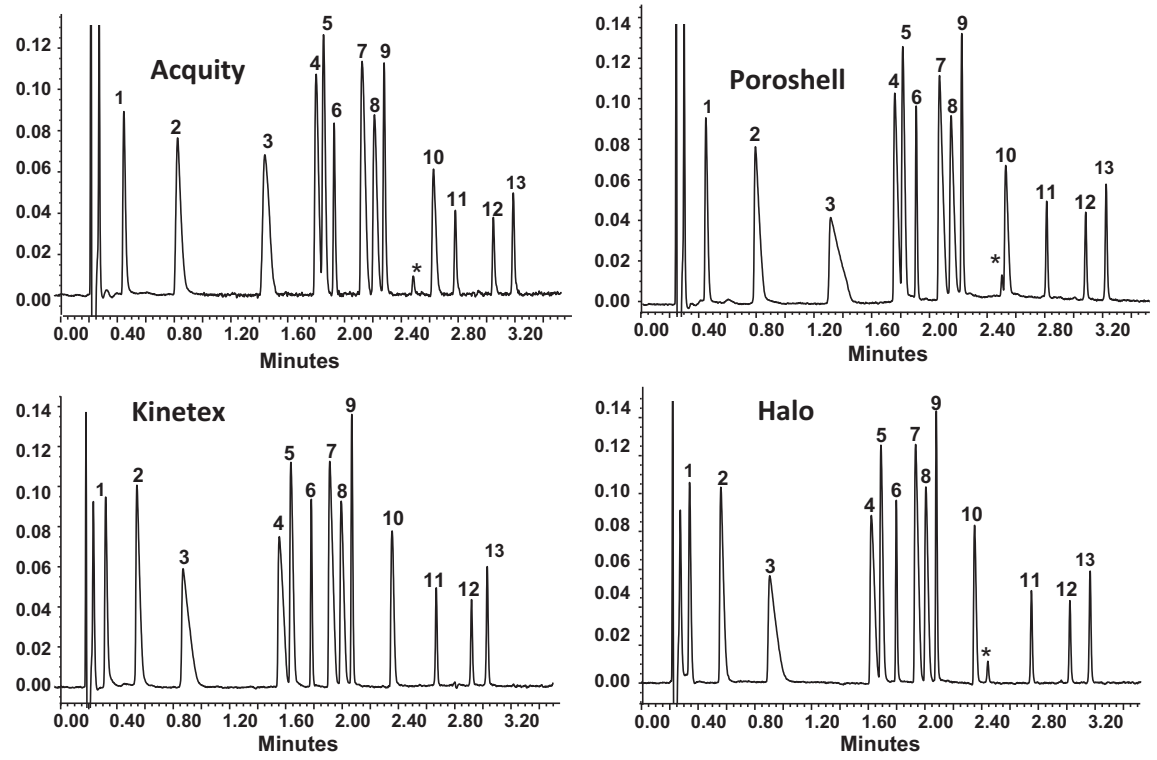

Fig. 4. Separation of 13 pharmaceutical compounds on Acquity BEH C18, 50 × 2.1 mm, 1.7 μm; Poroshell 120 EC-C18, 50 × 2.1 mm, 2.7 μm; Kinetex C18, 50 × 2.1 mm, 2.6 μm and Halo C18, 50 × 2.1 mm, 2.7 μm. *Conditions*: mobile phase: 0.1% formic acid in water modified with 0.1% formic acid in ACN, gradient profile: 5% ACN for 1 min, then 5–95% ACN in 3 min, flow rate of 500 μL/min, T = 40 °C, injected volume = 2 μL, λ = 230 nm. Elution order: (1) morphine 50 μg/mL, (2) atenolol 40 μg/mL, (3) codeine 100 μg/mL, (4) lidocaine 100 μg/mL, (5) prilocaine 50 μg/mL, (6) acebutolol 10 μg/mL, (7) bupropion 30 μg/mL, (8) bupivacaine 100 μg/mL, (9) propanolol 8 μg/mL, (10) trimipramine 50 μg/mL, (11) ketoprofen 12 μg/mL, (12) flurbiprofen 8 μg/mL, (13) ibuprofen 25 μg/mL. (*) designates an impurity present within the mixture.

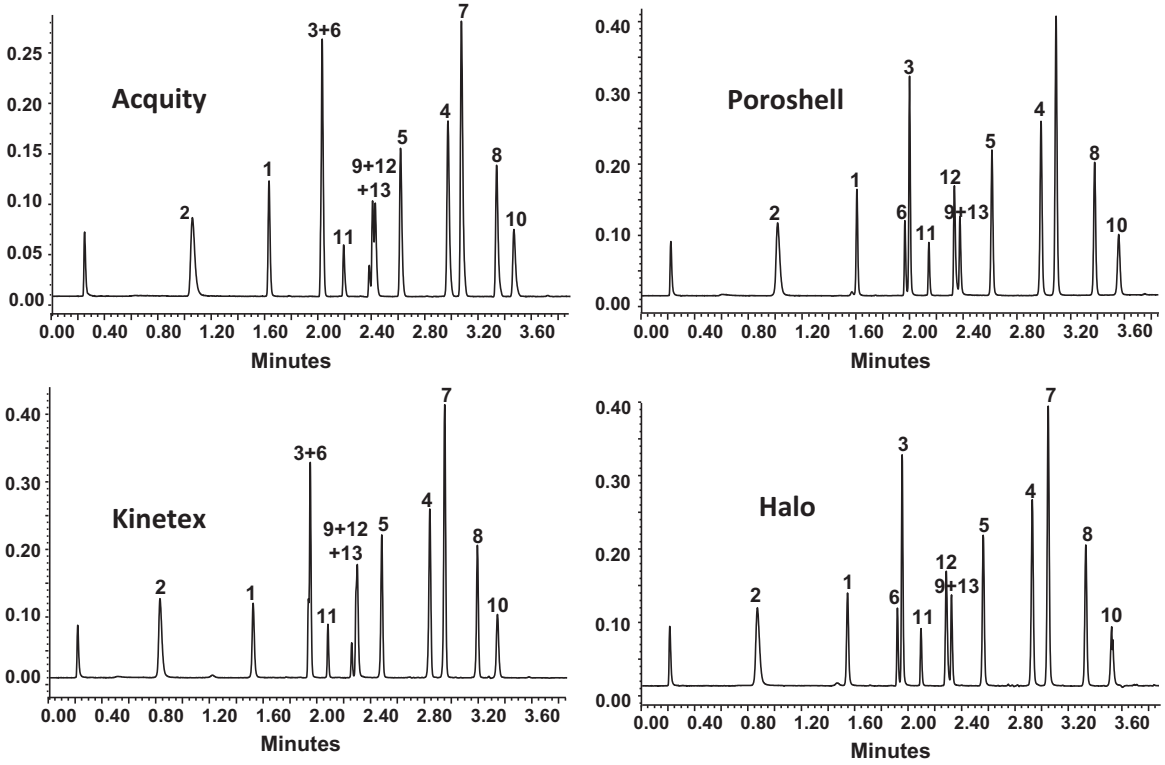

Fig. 5. Separation of 13 pharmaceutical compounds (same compounds as Fig. 4) on Acquity BEH C18, 50 × 2.1 mm, 1.7 μm; Poroshell 120 EC-C18, 50 × 2.1 mm, 2.7 μm; Kinetex C18, 50 × 2.1 mm, 2.6 μm and Halo C18, 50 × 2.1 mm, 2.7 μm. *Conditions*: mobile phase: phosphate buffer (20 mM, pH 6.85) modified with ACN, gradient profile: 5% ACN for 1 min, then 5–95% ACN in 3 min, flow rate of 500 μL/min, T = 40 °C, injected volume = 2 μL, λ = 230 nm. (*) designates an impurity present in the mixture.

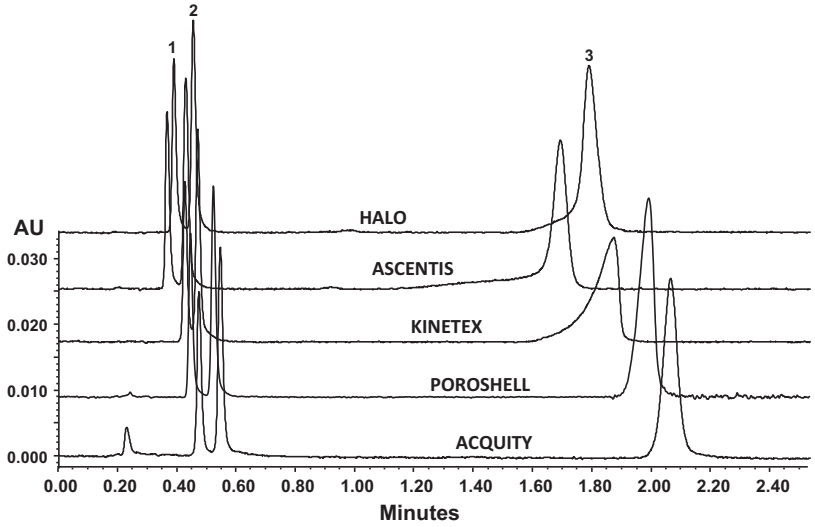

Fig. 6. Comparison of the retention capacity on different columns (Acquity BEH C18, 50 × 2.1 mm, 1.7 μm; Poroshell 120 EC-C18, 50 × 2.1 mm, 2.7 μm; Kinetex C18, 50 × 2.1 mm, 2.6 μm; Ascentis Express C18, 50 × 2.1 mm, 2.7 μm and Halo C18, 50 × 2.1 mm, 2.7 μm) for polar compounds ((1) sulfaguanidine, (2) sulfanilamide and (3) sulfadiazine at 50 μg/mL). *Conditions*: 0.1% formic acid in water modified with 0.1% formic acid in ACN, isocratic conditions: 2% ACN, flow rate of 500 μL/min, T = 40 °C, injected volume = 2 μL, λ = 230 nm.

section, kinetic plots were constructed by extrapolating the data obtained on a column of a given length to shorter or longer columns generating the maximal pressure drop that the chromatographic system could withstand. Previously, we emphasized that efficiency could strongly vary with column length; thus, kinetic plots were generated based on data obtained with 50 mm (Fig. 3A) and 150-mm column length (Fig. 3B).

As these two representations were very different, there is no interest in interpreting in details Fig. 3A and B. However, because kinetic plot representations were often constructed on the basis of extrapolation from a 50-mm column packed with shell particles (e.g., [21]), results should be considered with caution because the packing quality could depend on the column length and the provider, therefore, extrapolation is no longer valid.

3.4. Chromatographic behavior of columns packed with shell particles with compounds of pharmaceutical interest

Beside the kinetic performance, it is important to evaluate the chromatographic behavior of these new materials in real chromatographic conditions. Thus, a mixture of 13 relevant pharmaceutical compounds was investigated with a generic gradient in acidic and neutral conditions. The test mixture includes basic drugs with pK_a comprised between 7.2 and 9.5 as well as acidic compounds with pK_a ranging between 4.1 and 4.4. To reach acidic conditions (approximately pH 2.7), 0.1% formic acid was added to both aqueous and organic solvents of the mobile phase. For neutral conditions, 20 mM phosphate buffer (pH 6.85) was selected. Figs. 4 and 5 report chromatograms obtained with different columns packed with shell particles and sub-2-μm particles, in acidic and neutral pH, respectively. During this study, only C18 materials were tested, but other chemistries are available from different providers.

As reported in Fig. 4, the elution order remained strictly equivalent between the different columns. This was because residual silanols should be mostly neutral at pH 2.7, and retention was governed by a pure reversed phase mechanism. Selectivity between successive peak pairs was also very similar, except for morphine (peak 1), which was eluted more rapidly on Kinetex and Halo columns. Selectivity between prilocaine (peak 5)/acebutolol (peak 6) and also between lidocaine (peak 4)/prilocaine (peak 5) were reduced on the Acquity compared to the Kinetex column. In addition, selectivity between an unidentified impurity and trimipramine (peak 10) changed significantly between columns. Despite these small changes in selectivity, the overall separation, and thus, the hydrophobicity of the support remained nearly constant. Thus, if the method was originally developed on a fully porous material, such as the Acquity column, it could be transferred to columns packed with shell particles. However, some adjustments could be necessary to attain acceptable selectivity for the most critical peak pairs. Finally, peaks exhibited a similar symmetry and width on the different columns, except atenolol (peak 2), codeine (peak 3) and lidocaine (peak 4), which present a more or less pronounced tailing, depending on the considered column. This behavior could be related to the loading capacity of these different columns and is discussed in the next section.

In Fig. 5, the same separation of pharmaceutical compounds was performed at neutral pH. In these conditions, most of the residual silanols were in their deprotonated form because the pK_a of silanols are generally between 3.5 and 6.8 [22]. Because the tested compounds consisted of basic drugs, more pronounced changes in retention and selectivity were expected because silanol activity can vary between columns. The tailing previously observed on peaks 2, 3 and 4 was not anymore observed at neutral pH. Again, selectivity of the different columns was similar, even for the most critical pairs. A better separation of codeine (peak 3) and acebutolol (peak 6) was observed on Poroshell and Halo columns, while the Acquity column was not able to distinguish these compounds. On the contrary, the Acquity column was able to discriminate propranolol (peak 9), flurbiprofen (peak 12) and ibuprofen (peak 13). Because all columns packed with shell particles were end-capped, it was not surprising that silanol activity was very similar. Only small variations in the proprietary bonding process could explain the minor selectivity changes between these columns. Finally, the Acquity column was a hybrid, fully end-capped material with a lower acidity of surface silanols groups (pK_a > 8) [22]. This could explain the little difference in selectivity observed at neutral pH compared to columns packed with shell particles.

To conclude, shell particles presented selectivity very close to fully porous particles for our tested mixture. Thus, if a method should be transferred, only small adjustments should be applied to maintain constant retention and selectivity. However, even if some additional column chemistries are already available (i.e., C8, silica, phenyl, phenyl-hexyl, PFP, amide), the number of shell particles can

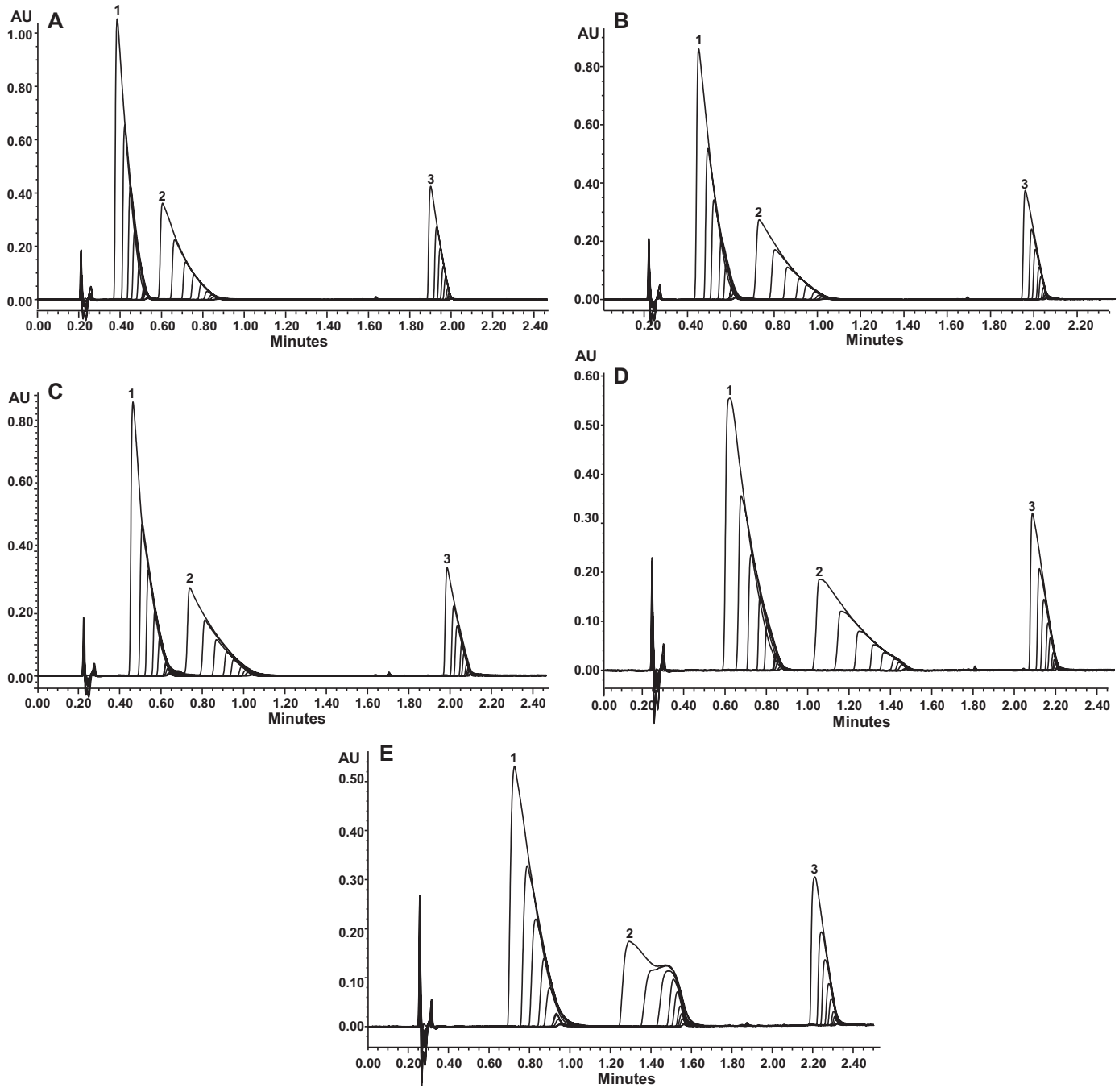

Fig. 7. Influence of the compounds concentration on the peak shape for the different columns ((A) Ascentis Express C18, 50 × 2.1 mm, 2.7 μm; (B) Halo C18, 50 × 2.1 mm, 2.7 μm; (C) Kinetex C18, 50 × 2.1 mm, 2.6 μm; (D) Poroshell 120 EC-C18, 50 × 2.1 mm, 2.7 μm and (E) Acquity BEH C18, 50 × 2.1 mm, 1.7 μm) for the analysis of (1) atenolol, (2) codeine and (3) bupivacaine at 1, 2, 5, 10, 20, 50, 100, 200, 500, and 1000 μg/mL. *Conditions*: 0.1% formic acid in water modified with 0.1% formic acid in ACN, gradient profile: 5% ACN for 1 min, then 5 to 95% ACN in 3 min, flow rate of 500 μL/min, T = 40 °C, injected volume = 2 μL, λ = 230 nm.

still be limited compared to fully porous UHPLC columns. Indeed, it could be interesting to have a C18 material with polar embedded group for the separation of isomers [23]; a less hydrophobic alkyl chain, such as C4 material for proteins analysis [24]; different HILIC phases (particularly a zwitterionic one) to deal with polar compounds [25]; and a cyano column to elute most apolar compounds within reasonable time frame.

3.5. Retention of columns packed with shell particles

Because of the solid inner core of shell particles, the latter can suffer from a lower retention in comparison with a fully porous particle of the same material. The porous shell volume (V_p), available for retention, can be easily calculated [3]:

$$V_p = \pi \frac{d_p^3 - d_i^3}{6} \quad (4)$$

where d_p and d_i are the diameter of the particle and the solid core, respectively. The geometry of Ascentis, Halo and Poroshell columns was strictly similar (d_p of 2.7 μm, d_i of 1.7 μm, shell thickness of 0.5 μm) and the fraction of porous shell corresponded to 75% of the total particle volume. For Kinetex particles (d_p of 2.6 μm, d_i of 1.9 μm, shell thickness of 0.35 μm), the porous layer corresponded

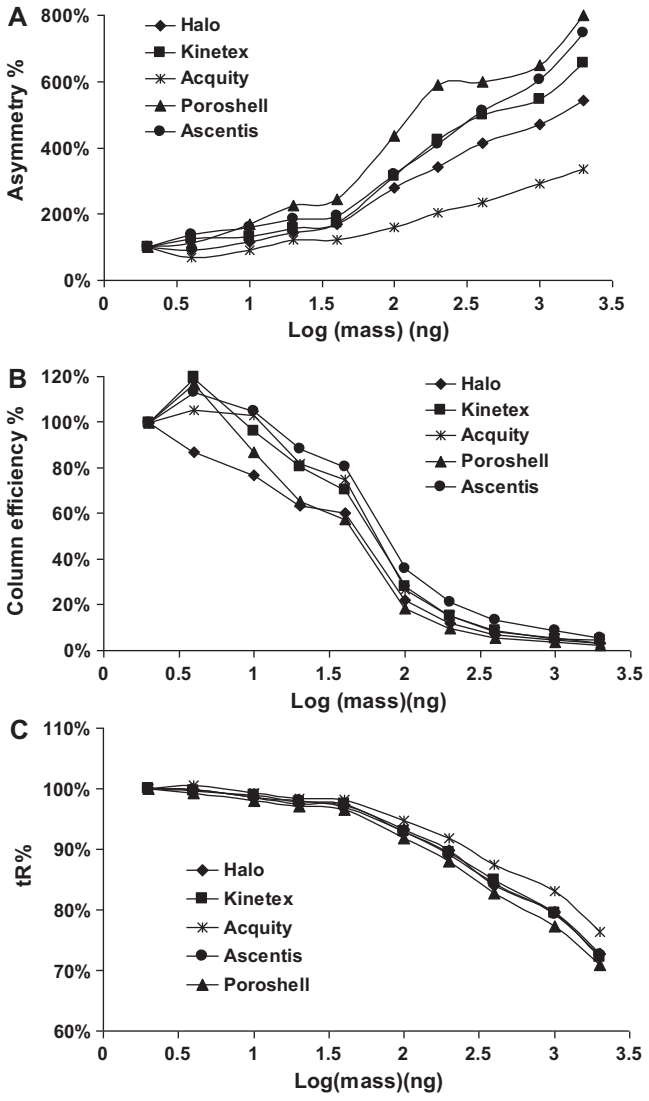

Fig. 8. Relative evolution of asymmetry (A), column efficiency (B) and retention factor (C) in function of the logarithm of the mass of atenolol at pH 3 with the different columns. *Conditions*: 0.1% formic acid in water modified with 0.1% formic acid in ACN, gradient profile: 5% ACN for 1 min, then 5 to 95% ACN in 3 min, flow rate of 500 μL/min, T = 40 °C, injected volume = 2 μL, λ = 230 nm.

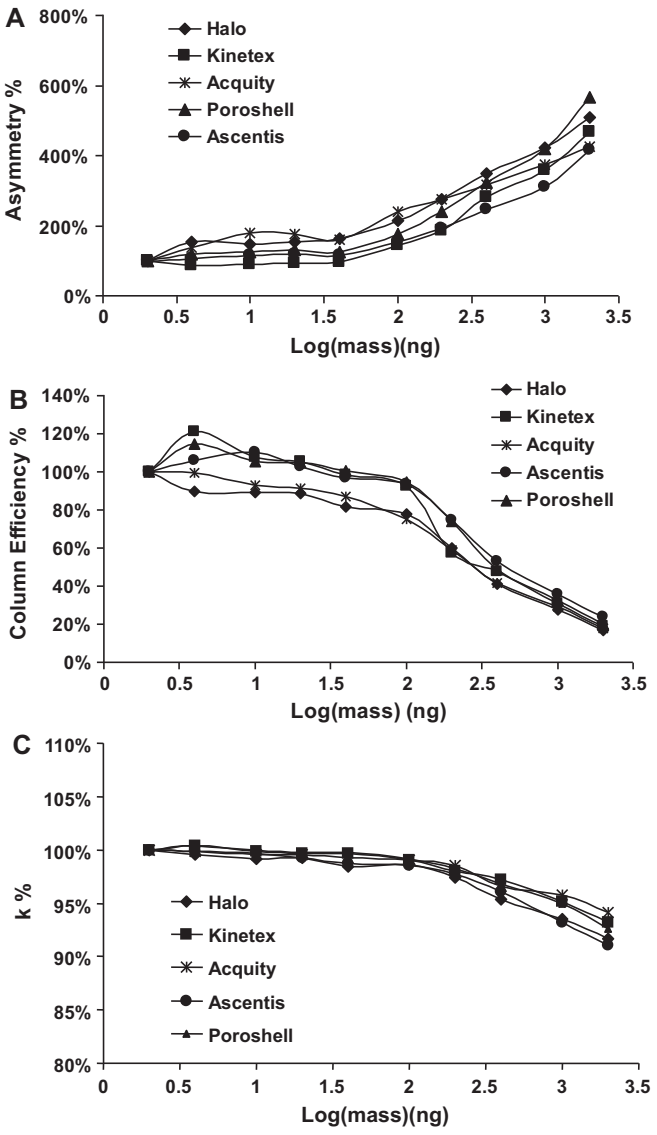

Fig. 9. Relative evolution of asymmetry (A), column efficiency (B) and retention time (C) in function of the logarithm of the mass of atenolol at pH 6.85 with the different columns. *Conditions*: mobile phase: phosphate buffer (20 mM, pH 6.85) modified with ACN, gradient profile: 5% ACN for 1 min, then 5–95% ACN in 3 min, flow rate of 500 μL/min, T = 40 °C, injected volume = 2 μL, λ = 230 nm.

to 64% of the total particle volume. Thus, the volume of the porous material within the column was significant.

To evaluate the ability of columns packed with shell particles to retain relatively polar compounds, a critical mixture of 3 antibacterial sulfonamides possessing $\log D_{pH3}$ values between −0.1 (sulfadiazine) and −1.3 (sulfaguanidine) was prepared and analyzed. The corresponding chromatogram is reported in Fig. 6. To calculate retention factors of the compounds, the column dead time was experimentally measured with uracil after the deduction of extra-column volume contribution (13 μL) and a system offset of 0.013 min. The t_0 were equal to 0.168, 0.178, 0.205, 0.183, 0.177 min for Ascentis, Kinetex, Acquity, Poroshell and Halo material, respectively. It is not surprising that the column dead time on columns packed with shell particles was lower as the porosity was reduced because of the solid inner core. As expected, the retention of these compounds on C18 material was very limited and required a mobile phase containing only 2% ACN. In these isocratic conditions, the retention factor for the early-eluted peak (i.e., sulfaguanidine) varied from 0.97 to 1.15 between the two most different columns (Ascentis and Acquity). For the last eluted peak (i.e., sulfadiazine), k was always equal to 8.9 for all investigated columns. To conclude, the decrease in retention factor between the UHPLC column packed with fully porous particles and columns packed with shell particles was equal to 15% (on the maximum) for the Ascentis column. Finally, retention factors on Poroshell were very similar to those obtained on Acquity, confirming that the surface available for retention on these shell particles was sufficient.

Finally, the retention of butylparaben, a more hydrophobic compound ($\log P$ = 3.41) than sulfonamides was also calculated, to evaluate the amount of hydrophobic binding sites on these different columns. It appears that the retention factor of this compound eluted with 35% ACN/65% water was comprised between 8.2 and 8.4 for the Halo, Ascentis and Acquity. On the other hand, the k value was around 10% lower for the Kinetex material and about 10% higher for the Poroshell one. These small differences can be explained by changes of carbon load, pore diameter, surface coverage between columns and also by the nature of the endcapping and the proprietary bonding process.

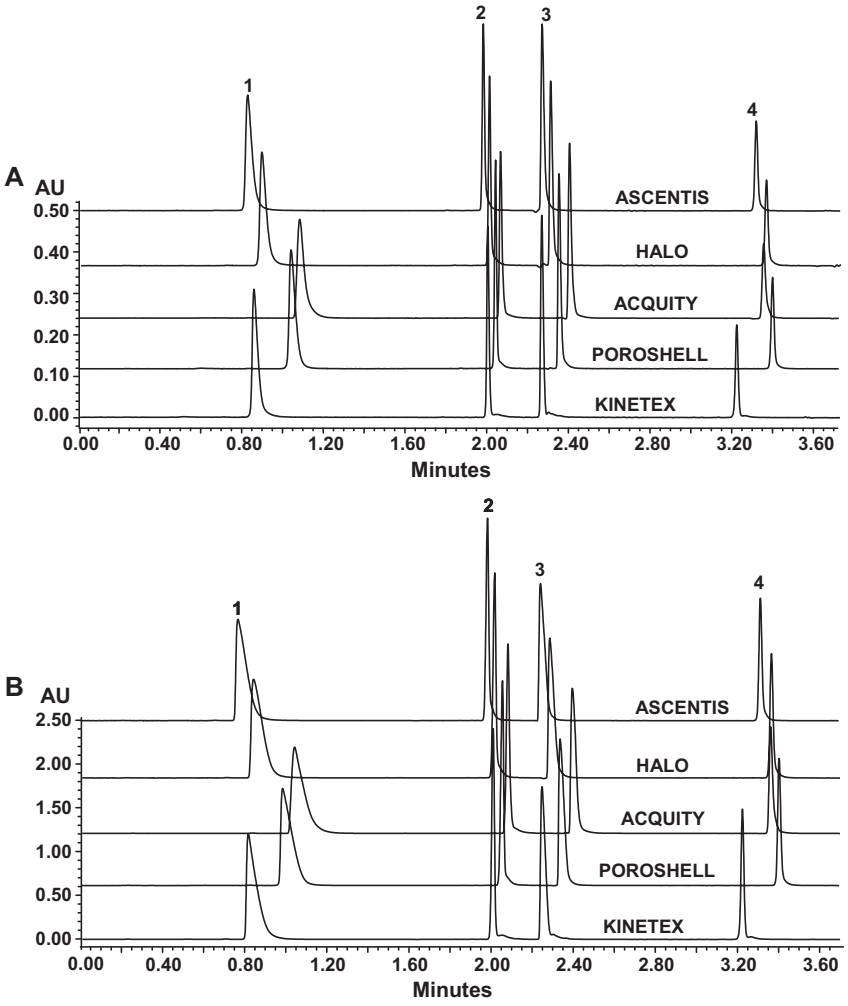

Fig. 10. Separation of a mixture of (1) atenolol, (2) codeine, (3) bupivacaine and (4) ibuprofen at 100 μg/mL (A) and 1000 μg/mL (B) on the different stationary phases at pH 6.85. *Conditions*: mobile phase: phosphate buffer (20 mM, pH 6.85) modified with ACN, gradient profile: 5% ACN for 1 min, then 5–95% ACN in 3 min, flow rate of 500 μL/min, T = 40 °C, injected volume = 2 μL, λ = 230 nm.

3.6. Loading capacity of columns packed with shell particles

Another possible issue related to the thickness of the porous layer was the loading capacity of the column. As calculated with Eq. (4), the volume fraction of the porous shell was quite important (75 and 64%, depending on the geometry), and thus, the loading capacity of the column should be acceptable.

To explore this parameter, three of the most critical compounds from the mixture of drugs (i.e., atenolol, codeine and bupivacaine) were employed in both acidic and neutral conditions. Investigated concentrations ranged from LOD (1 μg/mL) to a high concentration level (1000 μg/mL). Because of the large number of experiments required in this study, it was difficult to perform the analysis of individual compounds in the isocratic mode. Thus, experiments were conducted with a generic gradient. The initial 1 min isocratic step at 5% ACN allowed the elution of atenolol and sometimes codeine (on Ascentis, Halo, Kinetex), thus confirming that Acquity and Poroshell were slightly more retentive. However, bupivacaine was eluted during the gradient.

3.7. Overloading effects in acidic conditions (0.1% formic acid)

Fig. 7 presents the chromatograms obtained with the 5 different columns and for sample concentrations of 1, 2, 5, 10, 20, 50, 100, 200, 500 and 1000 μg/mL in acidic conditions. For each column, a characteristic band tailing was accompanied by a reduction of retention with increasing sample load. The most deleterious effect was observed for codeine and atenolol because they were often eluted in the isocratic mode, while the tailing on bupivacaine was less pronounced due to peak compression effects during the gradient run. A peak shouldering was observed for codeine on Acquity BEH at concentration levels higher than 200 μg/mL. To confirm this observation, experiments were duplicated using various Acquity BEH columns, and this behavior was systematically observed. This could be related to the fact that the start of the gradient corresponded precisely to the elution of codeine. This effect was also observed with Poroshell at the same retention time on the chromatogram, but in this case, the shouldering was less pronounced.

To better visualize overloading effects, asymmetry, column efficiency and retention factor were reported as a function of the injected sample mass, composed of 2 ng to 2 μg (Fig. 8), in agreement with studies of McCalley et al. [26,27]. Asymmetry, efficiency and retention factors observed for an injected mass of 2 ng were considered as the reference value (negligible overloading effect), and the relative loss for each sample mass was calculated and reported in Fig. 8. Because the inter-column behavior was quite similar for the 3 investigated compounds, only data of atenolol were reported because the latter was always eluted during the initial isocratic step (thus, efficiency and retention factors could be calculated). As expected, an increase in asymmetry by up to 8-fold was

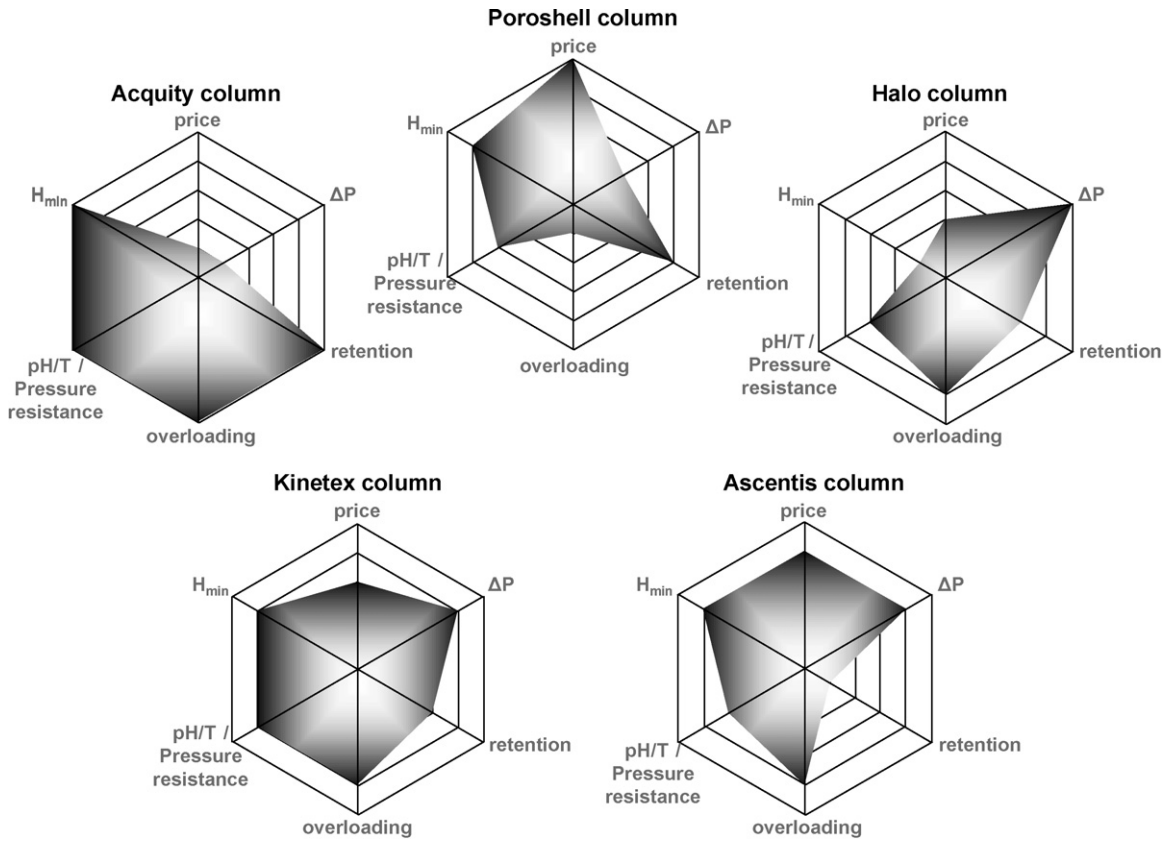

Fig. 11. Schematic comparison of the different column performance based on different parameters: price, resistance to pressure, retention and overloading capacity, pH/temperature/pressure resistance and minimal plate height values.

observed simultaneously with a reduction of up to 30% in retention factor and a diminution of efficiency by up to 50-fold in the worst case when the stationary phase overloaded. According to Fig. 8, the detrimental effects were observed for injected masses beyond 40 ng (equivalent to 20 ppm). Generally, there was a good correlation between the data obtained for asymmetry (Fig. 8A) and retention factor (Fig. 8C) and the column ranking was equivalent. Conversely, the evolution of efficiency loss for the different stationary phases (Fig. 8B) was more difficult to interpret, particularly for the lowest injected masses and this was certainly linked to the inaccurate measurement and the limited variation of efficiency at such low values. Because the increase of asymmetry and reduction of retention factor was always less pronounced for the fully porous Acquity column, the latter was less subjected to mass overloading effects. Regarding columns packed with shell particles more prone to overloading than Acquity material, Halo, Ascentis and Kinetex materials were not significantly different, while Poroshell was the most critical. At first, results obtained for the different shell particles were quite unexpected because the loading capacity should be theoretically proportional to the shell thickness, and thus, the Kinetex column should be the most critical. This confirmed that the shell thickness was not the only parameter for explaining loading capacity and that the carbon load, surface chemistry, pore size, surface area, surface coverage, end-capping nature and bonding process could play an important role.

Two mechanisms have been proposed in the literature to explain the overloading of basic drugs in acidic conditions, which generate tailed peaks and significant loss in efficiency: (i) Guiochon et al. [28] proposed that the tailing observed with silica-based stationary phases could be related to the presence of few strong sites of high adsorption energy among a huge number of sites with low adsorption energy. Band tailing could result either from rapid overload of the strong sites or from the slower sorption/desorption of basic drugs from these sites. However, it was demonstrated that there were very few (if any) ionized silanols on type B silica phases at acidic pH [29]. Furthermore, a hybrid material, such as Acquity BEH, was expected to contain even less ionized silanols considering the high pK_a value. (ii) Stahlberg et al. [30] and McCalley [31,32] suggested that positively charged drug interacts with C18 alkyl chains (hydrophobic interaction). Thus, the initially adsorbed charged molecules discourage further sorption of molecules possessing the same charge (electrostatic repulsion). Some additional experiments were conducted with the Acquity stationary phase (i.e., increase of mobile phase temperature, variation of pore size from 120 to 300 A, change from Acquity to Acquity Shield stationary phase). All of these tests helped us to conclude that the second mechanism was certainly the correct one.

Because the overloading can be explained in our case by a mutual repulsion of similarly charged analytes at the surface of the bonding chains, it is likely that specific parameters such as the pore volume or surface coverage (C18 only) were involved in overloading phenomenon. In this case, overloading would increase with a decrease in the amount of C18 chains accessible to ionized solutes. As it is difficult to determine precisely this amount, we can just suppose that it might be smaller on the Kinetex material, considering both pore diameter and surface coverage (100 Å and 2.7 μmol/m^2) compared to the Acquity BEH column (130 Å and 3.1 μmol/m^2).

3.8. Overloading effects in neutral conditions (20 mM phosphate buffer)

The same experiments were conducted at neutral pH. In these conditions, the loading capacity was improved compared to acidic pH on the same columns, as reported in Fig. 9. The asymmetry

increased by up to 6-fold (Fig. 9A) with a reduction of up to 6% in retention factor (Fig. 9B) and a diminution of efficiency by up to 5-fold (Fig. 9C) in the worst case. The improvement of peak shape with basic drugs on the silica-based stationary phase in neutral *vs*. acidic pH conditions was also reported by McCalley [11]. In acidic conditions, the number of residual silanols was quite limited, and thus, interactions of protonated basic solutes with the stationary phase were primarily hydrophobic. Conversely, silanols were deprotonated at neutral pH values, while basic drugs were primarily positively charged. Thus, hydrophobic and ion-exchange mechanisms occurred simultaneously, generating a higher number of interaction sites at the surface of the stationary phase, thus improving the loading capacity of the column. At neutral pH, it became extremely difficult to rank the columns because observed differences in terms of asymmetry, efficiency and retention factor were very small. In conclusion, no obvious difference was observed between columns packed with fully porous and shell particles, but it was always beneficial to work in neutral pH conditions when analyzing basic drugs.

Finally, Fig. 10 shows chromatograms of a mixture of 4 compounds (i.e., 3 basic drugs and 1 acidic drug) on the 5 different columns at two concentrations levels. For a concentration of 1000 μg/mL (Fig. 10B), peaks were distorted, while for a concentration of 100 μg/mL (Fig. 10A), peaks were more symmetrical. Similar chromatograms were also obtained in acidic conditions (data not shown), but a concentration equal to or below 10 μg/mL should be employed to reach an acceptable peak shape, confirming that the loading capacity of all tested columns was strongly enhanced at higher pH and higher ionic strength.

During our current study, McCalley also investigated the overloading behavior of sub-2-μm porous and sub-3-μm shell particles, but only Halo and Kinetex were investigated [11]. In this study, a slight reduction of loading capacity was highlighted and attributed to the non-porous core of the particle (down to 60% for the Kinetex). Similar to our conclusions, formic acid buffer (pH 2.7) was not recommended because it decreased efficiency by twofold compared to ammonium formate and potassium phosphate buffers.

4. Conclusion

In the present study, the applicability of columns packed with shell particles was evaluated using typical conditions found in the pharmaceutical industry. In our opinion, the kinetic performance of this new technology is extremely promising because h_{opt} values below 2 were attained for neutral compounds; even if the calculation of h_{opt} was somewhat questionable because of the special morphology of the shell particles. Numerous additional parameters should be considered to adequately select the best column, including the price, generated backpressure, H_{opt} value, retention capability, loading capacity and pH/temperature/pressure resistance. To select the best column for a given application, all of these figures of merits have been combined in the spidergrams of Fig. 11 for the 5 investigated columns.

According to the present study, columns packed with sub-3-μm shell particles combined with a chromatographic system that withstand pressures of 600 bar could be a valuable alternative to UHPLC system because it allows the possibility to obtain a very similar performance with limited frictional heating effects [11,33]. However, this new shell particles technology should only be employed on an optimized chromatographic system, where the extra-column and the system dwell volumes are reduced, as reported elsewhere [34,35].

There are numerous ways to improve the current version of columns packed with core–shell particles:

(1) The packing procedure for 2.1 mm I.D. columns could be improved as h_{opt} values of 1 to 1.3 were reported for columns of 4.6 mm I.D.
(2) According to this study, the inter-batch variability should be reduced and the packing of longer columns could be improved to reach h_{opt} values similar to shorter columns.
(3) The chemical (i.e., pH resistance) and also mechanical resistance (i.e., maximal temperature and backpressure) should be improved. We expect to have columns packed with shell particles that withstand pressure of 1000 bar very soon.
(4) The choice in terms of column chemistry is still limited compared to fully porous UHPLC columns and it would be valuable to have C18 material with polar embedded groups, C4 material, cyano bonding and additional choice for HILIC mode.

Acknowledgments

The authors wish to thank Dr. Raul Nicoli for stimulating discussions, and valuable comments.

References

[1] J.M. Cunliffe, T.D. Maloney, J. Sep. Sci. 30 (2007) 3104.
[2] J. Ruta, D. Guillarme, S. Rudaz, J.L. Veuthey, J. Sep. Sci. 33 (2010) 2465.
[3] F. Gritti, G. Guiochon, J. Chromatogr. A, 1218 (2011) 1915.
[4] J.J. Kirkland, Anal. Chem 64 (1992) 1239.
[5] A. Staub, D. Guillarme, J. Schappler, J.L. Veuthey, S. Rudaz, J. Pharm. Biomed. Anal. 55 (2011) 810.
[6] J.J. Destefano, T.J. Langlois, J.J. Kirkland, J. Chromatogr. Sci. 46 (2008) 254.
[7] F. Gritti, A. Cavazzini, N. Marchetti, G. Guiochon, J. Chromatogr. A 1157 (2007) 289.
[8] E. Olah, S. Fekete, J. Fekete, K. Gazler, J. Chromatogr. A 1217 (2010) 3642.
[9] F. Gritti, I. Leonardis, D. Shock, P. Stevenson, A. Shalliker, G. Guiochon, J. Chromatogr. A 1217 (2010) 1589.
[10] F. Gritti, G. Guiochon, J. Chromatogr. A 1217 (2010) 8167.
[11] D.V. McCalley, J. Chromatogr. A 1218 (2011) 2887.
[12] G. Desmet, P. Gzil, D. Nguyen, D. Guillarme, S. Rudaz, J.L. Veuthey, N. Vervoort, G. Torok, D. Cabooter, D. Clicq, Anal. Chem. 78 (2006) 2150.
[13] D. Guillarme, S. Heinisch, J.L. Rocca, J. Chromatogr. A 1052 (2004) 39.
[14] http://www.vub.ac.be/CHIS/Research/kp/kp_analyser/KineticPlotAnalyser.html (consulted in August 2011).
[15] G. Desmet, P. Gzil, D. Clicq, LC–GC Eur. 18 (2005) 403.
[16] F. Gritti, G. Guiochon, J. Chromatogr. A 1166 (2007) 30.
[17] F. Gritti, I. Leonardis, J. Abia, G. Guiochon, J. Chromatogr. A 1217 (2010) 3819.
[18] F. Gritti, G. Guiochon, J. Chromatogr. A 1218 (2011) 907.
[19] D. Cabooter, A. Fanigliulo, G. Bellazzi, B. Allieri, A. Rottigni, G. Desmet, J. Chromatogr. A 1217 (2010) 7074.
[20] S. Fekete, K. Ganzler, J. Fekete, J. Pharm. Biomed. Anal. 54 (2011) 482.
[21] E. Olah, S. Fekete, J. Fekete, K. Ganzler, J. Chromatogr. A 1217 (2010) 3642.
[22] K.D. Wyndham, J.E. O'Gara, T.H. Walter, K.H. Glose, N.L. Lawrence, B.A. Alden, G.S. Izzo, C.J. Hudalla, P.C. Iraneta, Anal. Chem. 75 (2003) 6781.
[23] D. Guillarme, C. Casetta, C. Bicchi, J.L. Veuthey, J. Chromatogr. A 1217 (2010) 6882.
[24] A. Staub, D. Zurlino, S. Rudaz, J.L. Veuthey, D. Guillarme, J. Chromatogr. A 1218 (2011) 8903.
[25] J. Ruta, S. Rudaz, D.V. McCalley, J.L. Veuthey, D. Guillarme, J. Chromatogr. A 1217 (2010) 8230.
[26] J. Dai, P.W. Carr, D.V. McCalley, J. Chromatogr. A 1216 (2009) 2474.
[27] D.V. McCalley, J. Chromatogr. A (1998) 31.
[28] T. Fornstedt, G. Zhong, G. Guiochon, J. Chromatogr. A 741 (1996) 1.
[29] A. Mendez, E. Bosch, M. Roses, U.D. Neue, J. Chromatogr. A 986 (2003) 33.
[30] I. Häglund, J. Stahlberg, J. Chromatogr. A 761 (1997) 3.
[31] D.V. McCalley, J. Chromatogr. A 1217 (2010) 858.
[32] S.M.C. Buckenmaier, D.V. McCalley, M.R. Euerby, Anal. Chem. 74 (2002) 4672.
[33] L. Novakova, J.L. Veuthey, D. Guillarme, J. Chromatogr. A 1218 (2011) 7971.
[34] F. Gritti, C.A. Sanchez, T. Farkas, G. Guiochon, J. Chromatogr. A 1217 (2010) 3000.
[35] D.V. McCalley, J. Chromatogr. A 1217 (2010) 4561.